

See discussions, stats, and author profiles for this publication at: <https://www.researchgate.net/publication/266083005>

Immobilization of Proteins in their Physiological Active State at Functionalized Thiol Monolayers on ATR-Germanium Crystals

ARTICLE *in* CHEMBIOCHEM · NOVEMBER 2014

Impact Factor: 3.09 · DOI: 10.1002/cbic.201402478

CITATIONS

3

READS

43

7 AUTHORS, INCLUDING:



[Jonas Schartner](#)

Ruhr-Universität Bochum

9 PUBLICATIONS 24 CITATIONS

SEE PROFILE



[Konstantin Gavriljuk](#)

Max Planck Institute of Molecular Physiology

5 PUBLICATIONS 32 CITATIONS

SEE PROFILE

Immobilization of Proteins in their Physiological Active State at Functionalized Thiol Monolayers on ATR-Germanium Crystals

Jonas Schartner,^[a] Konstantin Gavriljuk,^[a] Andreas Nabers,^[a] Philipp Weide,^[b] Martin Muhler,^[b] Klaus Gerwert,^[a] and Carsten Kötting^{*,[a]}

Protein immobilization on solid surfaces has become a powerful tool for the investigation of protein function. Physiologically relevant molecular reaction mechanisms and interactions of proteins can be revealed with excellent signal-to-noise ratio by vibrational spectroscopy (ATR-FTIR) on germanium crystals. Protein immobilization by thiol chemistry is well-established on gold surfaces, for example, for surface plasmon resonance. Here, we combine features of both approaches: a germanium surface functionalized with different thiols to allow specific immobilization of various histidine-tagged proteins with over 99% specific binding. In addition to FTIR, the surfaces were characterized by XPS and fluorescence microscopy. Secondary-structure analysis and stimulus-induced difference spectroscopy confirmed protein activity at the atomic level, for example, physiological cation channel formation of Channelrhodopsin 2.

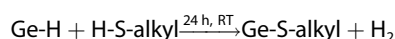
Protein immobilization is an important tool for biophysical investigations. It is the basis for many extensively applied techniques, such as protein microarrays and surface plasmon resonance (SPR). In protein microarrays, which can be read out with very high sensitivity by fluorescence spectroscopy,^[1–3] the requirement for dyes is a disadvantage; thus, label-free methods are becoming increasingly popular, as no interference is caused by the label molecules. SPR is often based on gold chips with commercially available functionalized chemical groups, so measurements are convenient to perform.^[4–6] However, SPR lacks spectral information, so yields kinetic and thermodynamic data but no chemical information. Spectral information is essential for understanding protein function at the atomic level; attenuated total reflectance Fourier transform infrared (ATR-FTIR) spectroscopy provides spectral information in real time and does not require labeling. Conformational changes, protein reactions, protein interactions with ligands, drugs, or other proteins can be investigated, and information

on protein orientation and secondary structure can be obtained.^[7–14] Previously, we reported protein immobilization on lipid bilayers,^[11,15] although lipid bilayers provide an environment that is close to that in vivo, their reusability is limited, and analysis of solubilized transmembrane proteins is impossible.

Chemically modified surfaces have huge potential, because many different chemical groups can be generated, and proteins can be investigated with different tags or chemical labels.^[16–18] Recently, we developed a chemically modified germanium surface with novel silanes and studied the activity of several proteins at high resolution.^[14] Conventionally, gold surfaces are functionalized with thiols for protein immobilization,^[19–21] but chemical modification of germanium with thiols was shown to be possible, although this has not been optimized for protein attachment.^[22–28] Germanium is well suited as an internal reflection element for ATR-FTIR spectroscopy because it has a high refractive index, which leads to an excellent signal-to-noise (s/n) ratio when using multiple reflections.^[29] A further advantage is the large spectral window (4000 to 900 cm^{−1}), which is essential for studying the sulfate and phosphate regions (not accessible with silicon internal reflection elements).^[14] Our flow-through cuvette method allows almost unlimited choice of chemicals and buffer solutions, and self-assembly of the thiol monolayer, chemical functionalization, and protein immobilization can be performed at room temperature.


Here, we report the assembly of a functionalized thiol monolayer on germanium for specific immobilization of histidine-tagged proteins. Protein immobilization on thiol-modified germanium is now accessible for the first time (Scheme 1). First, we followed the assembly steps of the surface by using ATR-FTIR spectroscopy and X-ray photoelectron spectroscopy (XPS). Then, several proteins were bound in their physiologically active states, ranging from the small GTPase N-Ras to the fluorescent protein mCherry, the transmembrane protein Channelrhodopsin 2 (ChR2), and phosphocholine transferase AnkX.

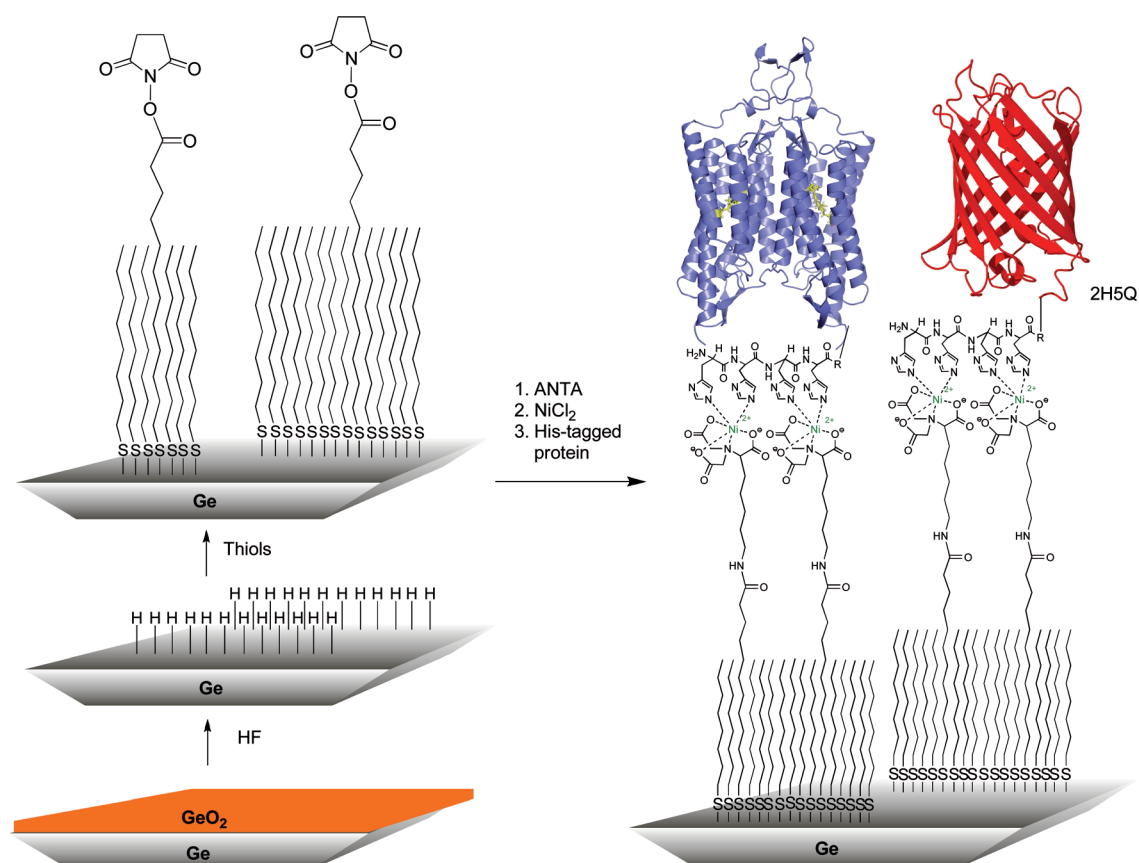
First, the germanium crystal was treated with hydrofluoric acid (HF) to generate a hydrogen-terminated surface.^[25] (Choi and Buriak describe hydrogen termination as a kinetic product; fluoride termination would be thermodynamically favorable.)^[30] After HF treatment, the crystal was incubated for 24 h in propan-2-ol containing the desired thiol.



[a] J. Schartner, Dr. K. Gavriljuk, A. Nabers, Prof. Dr. K. Gerwert, Dr. C. Kötting
Department of Biophysics, Faculty of Biology and Biotechnology
Ruhr-University Bochum
Universitätsstrasse 150, 44801 Bochum (Germany)
E-mail: carsten.koetting@rub.de

[b] P. Weide, Prof. Dr. M. Muhler
Laboratory of Industrial Chemistry, Faculty of Chemistry and Biochemistry
Ruhr-University Bochum
Universitätsstrasse 150, 44801 Bochum (Germany)

 Supporting information for this article is available on the WWW under <http://dx.doi.org/10.1002/cbic.201402478>.



Scheme 1. Assembly of a functionalized thiol-monolayer for the specific attachment of proteins, for example Channelrhodopsin 2 (shown in blue, homology model)^[35] or mCherry (red).

The proposed reaction mechanism is similar to adsorption on gold, and has been previously been described.^[19,28] The high stability of the GeS-alkyl surface is consistent with the stability of GeS compounds.^[31]

We used octanethiol, 3-mercaptopropanol, and 8-mercaptododecanol as unreactive lateral spacer molecules and 12-mercaptododecanoic acid N-hydroxysuccinimide ester (NHS-thiol) as the amine reactive linker. We followed the reaction of the NHS-thiol with amino-nitrilotriacetic acid (ANTA), and three new bands in the C–H region at were detected (2960, 2920, and 2852 cm^{-1}); these increased in intensity over time (Figure 1A). The positive bands at 1650 and 1540 cm^{-1} can be assigned as amide I and amide II of the new peptide bond formed between ANTA and the linker thiol; the stretching mode at 1409 cm^{-1} is caused by the deprotonated carboxylates from the ANTA head group; and the negative bands at 1728 and 1780 cm^{-1} are related to the reacted succinimide ring, which is substituted during the reaction (Figure 1B). Kinetic analysis was achieved by plotting the C–H band (asymmetric stretching mode) at 2960 cm^{-1} against time (note: this is not a stoichiometric reaction because the NHS ester can be hydrolyzed in a side reaction). The reaction with ANTA took about 100 min (fitted by a mono-exponential function), and resulted in a complete layer (Figure 1C). Unbound ANTA was then removed by washing, Ni^{2+} was added, unspecific binding sites were blocked (3 μM casein), and the desired

buffer was employed. The selection of buffer compositions or other chemicals with this surface is almost limitless, thus enabling measurements over a wide pH range or with detergents. A further general advantage is the use of thiols, as a huge range of different functionalized thiols is commercially available.

In addition to FTIR, the NHS-thiol modified (Figure 2A, top) and Ni-NTA-loaded germanium crystals (Figure 2A, bottom) were characterized by XPS (Supporting Information). HF treatment of germanium removes the GeO_2 layer completely, whereas GeO remains stable in all surfaces (Figure S1 and Table S1). GeO is known to desorb completely at 450 $^\circ\text{C}$.^[32] The removal of the GeO_2 layer is crucial for the assembly of thiol monolayers.^[27]

The peak positions for NHS-thiol modified surface are in good agreement with previously reported binding energies of similar compounds.^[14,33]

The peak shape of the C 1s signal (C1, C2, C3, C4) alters slightly upon ANTA modification (Figure 2A, bottom). In addition, a significant Ni 2p signal with the main Ni 2p_{3/2} peak at 856.3 eV was observed for a 100% Ni-NTA-modified sample (Supporting Information and Figure S2). Furthermore, the atomic concentrations from the experimental data of both surfaces fit the theoretical values very well (Table S2). Thus, the successful reaction of succinimide esters with ANTA and Ni^{2+} was confirmed by XPS measurement.

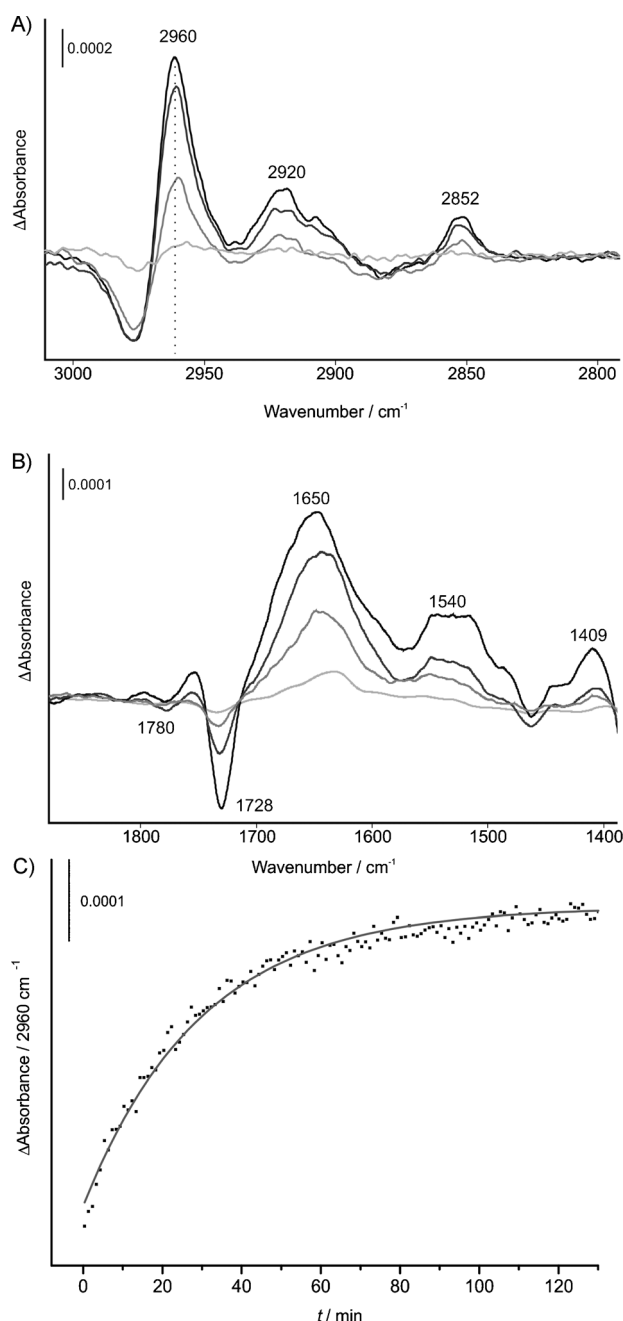


Figure 1. A) Reaction of the succinimidyl ester with amino-nitrilotriacetic acid (ANTA) monitored by C–H stretching modes (2960, 2920, 2852 cm⁻¹) and B) by the amide I (1650 cm⁻¹), amide II (1540 cm⁻¹), and carboxylate (1409 cm⁻¹) bands. C) The kinetics of the reaction were analyzed by plotting the C–H stretching band (2960 cm⁻¹) against time; —: 0, —: 25, —: 60, —: 90 min. The reaction was complete after about 100 min (fitted with a mono-exponential function; the surface was assembled with 50% NHS-thiol and 50% octanethiol).

A detailed characterization of the surface is presented in the Supporting Information. Briefly, the surface (20% NHS-thiol and 80% octanethiol) is stable at pH 3 and 13 for at least 24 h (Figure S3). Furthermore, polarized FTIR measurements indicated a well-packed monolayer with octanethiol and a worse-packed monolayer with 8-mercaptooctanol (see the section “Surface Characterization” and Figure S4 in the Supporting Information).

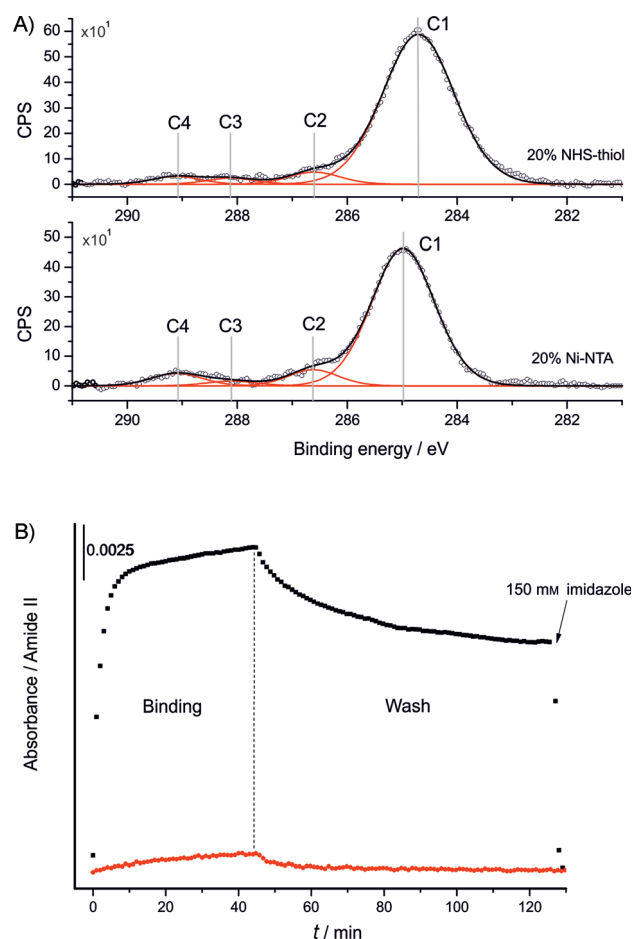


Figure 2. A1) XPS C 1s signal of a germanium surface modified with 20% NHS-thiol (A2) and the same crystal after further modification with Ni-NTA. (A1, A2) C1 corresponds to carbon in an alkyl chain (C–C, C–H), C2 is due to α-carbons adjacent to carbonylic carbons (C–CONR, C–COOR) and C3 and C4 were assigned to carbonylic carbon atoms in C–C(O)–NR and C–C(O)–OR species, respectively. B) Immobilization of N-Ras on a thiol monolayer containing 20% Ni-NTA head groups (■). Rinsing the surface with 150 mM imidazole leads to almost complete removal of the protein, thus indicating specific binding. In agreement, a surface that was treated with ethanolamine instead of ANTA (●) resulted in almost no unspecific binding (< 1%).

The stability of the protein N-Ras was analyzed on surfaces composed of various lateral spacer thiols. The most favorable surface had 20% Ni-NTA and 80% octanethiol: about 75% of the immobilized N-Ras molecules remained natively folded after 43 h (Figure S5). To study the protein binding, we used N-Ras with a decahistidine tag. N-Ras (final concentration 1 μM) was added to the flow-through system. To determine the ideal Ni-NTA concentration on the surface, different concentrations of 12-mercaptododecanoic acid NHS ester were reacted with ANTA: the ideal concentration for surface loading and stability was 20% Ni-NTA groups and 80% octanethiol (Figure S6). The kinetics of N-Ras immobilization showed fast binding over the initial 5 min with a maximum after 45 min at 16.5 mOD. The exponential binding kinetics hints at specific binding, as unspecific binding kinetics are often linear.^[14] In the next step, the surface was washed for at least 1 h to remove loosely bound protein and to check the stability of bound N-Ras

(black dots, Figure 2B). To assess the specificity of the germanium surface, the NHS groups were reacted with ethanolamine, and the same amount of N-Ras was added to the system. Only limited unspecific interactions occurred, and these were completely reversible (red dots, Figure 2B). Thus, we estimate the specificity of the surface to be about 99%. Furthermore, we tested the specificity with imidazole to determine the extent of unspecific binding. Imidazole treatment removed immobilized protein almost completely (unspecific binding $\sim 1\%$; Figure 2B). Imidazole affinity was determined as previously described^[18] (protein dissociation kinetics at 1–100 mM imidazole in Figure S7A). The amount of protein that could not be removed was plotted against imidazole concentration and was fitted to estimate an EC_{50} value of 13.3 mM (Figure S7B), in agreement with a previous evaluation (13.8 mM).^[18] This high stability can be explained by multivalent binding with several Ni-NTA groups, because one Ni-NTA group can interact with only two histidines. (All proteins in this study had at least a hexahistidine tag.)

The high specificity enables the analysis of the protein and its activity upon stimulation. Therefore, an activity assay using beryllium fluoride (BeF_x) was performed.^[34] The N-Ras protein functions as a molecular switch, being switched on by GTP binding and switched off upon GDP binding. BeF_x binds to Ras-GDP, and thereby mimics the GTP state. N-Ras was immobilized in the GDP state and a BeF_x titration was performed. We estimated the dissociation constant of BeF_x to be 2.1 ± 0.2 mM (Figure S8). In comparison with N-Ras immobilized on Ni-NTA silanes, the same difference spectrum is obtained (Figure S8B).^[14]

To further study the surface, the fluorescent protein mCherry with an N-terminal hexahistidine tag was applied. The binding kinetics show that mCherry at $1.8 \mu\text{M}$ binds as fast as N-Ras and remains stable at 11.5 mOD (parallel polarized IR, Figure 3A). In a control fluorescence measurement before the attachment, almost no fluorescence was detected (Figure 3B). After the addition of mCherry and a washing step to remove surplus mCherry, very strong fluorescence was observed (Figure 3B and C). Treatment with 150 mM imidazole removed almost all protein, and a 4000-fold fluorescence decrease was observed. The unspecific binding of inactive protein in this assay was less than 0.025%. We showed, within the resolution of the fluorescence microscope, that a homogenous protein layer had formed (Figure 3). This assay demonstrates that the protein was immobilized in a native state. The combination of ATR-FTIR with fluorescence microscopy is thus a useful technique to analyze protein activity.

To exclude denaturation of protein, we performed secondary-structure analysis (Supporting Information). The results are consistent with the X-ray data and confirm the natural fold of the protein (Table S3 and Figure S9). The surface concentrations of protein indicates a monolayer in all cases (Table S4)

We also immobilized phosphocholine transferase AnkX ($1 \mu\text{M}$) from *Legionella pneumophila* with a decahistidine tag as proof of principle for the study of soluble enzymes (Figure S10A). AnkX catalyzes the transfer of a phosphocholine moiety to the small GTPases Rab1 and Rab35 from CDP-chol-

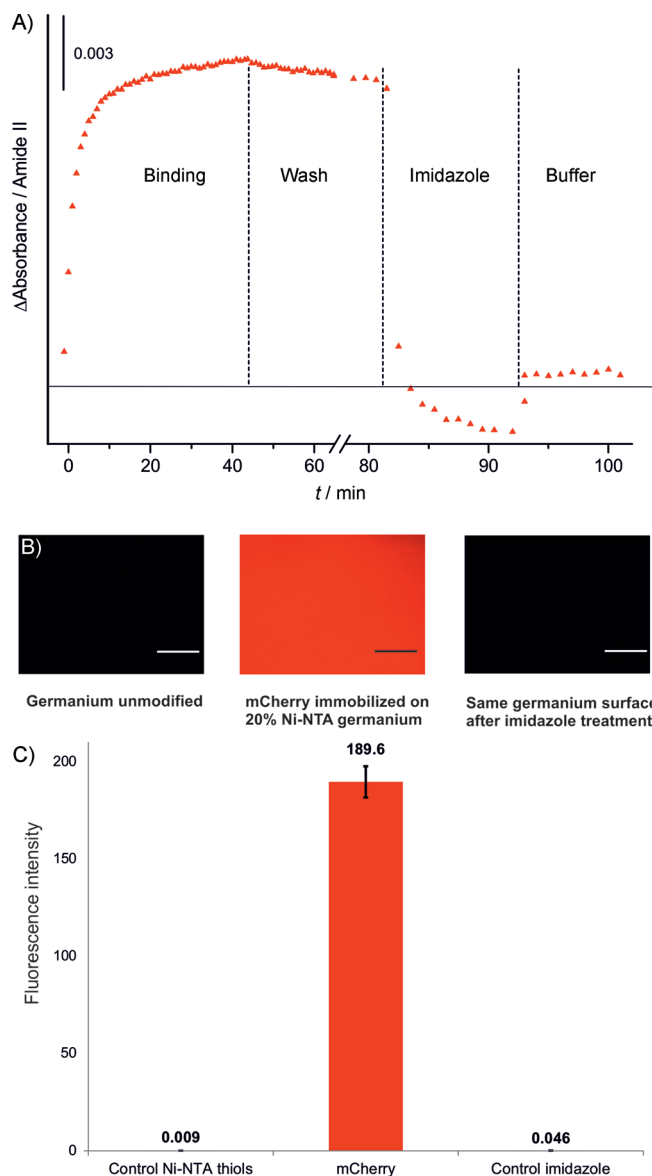


Figure 3. A) Binding kinetics of histidine-tagged mCherry to a 20% Ni-NTA surface. B) Fluorescence images before and after protein attachment, and after imidazole treatment; Scale bars: $200 \mu\text{m}$. C) The very low fluorescence yields in the controls underline the high specificity of the surface and show that the protein is immobilized in a native state.

ine (substrate). The difference spectrum revealed substrate-induced changes in AnkX (Figures S10B and S11).

Finally, Channelrhodopsin 2 ($1.3 \mu\text{M}$) with a C-terminal decahistidine tag in β -decylmaltoside micelles was immobilized at pH 7.4. After a washing step to remove loosely bound protein, the amide II band remained stable at about 12 mOD (parallel polarized IR, Figure 4A). To study the orientation of the protein, we performed dichroic ATR-FTIR measurements (Supporting Information). A positive band in the amide I region at 1658 cm^{-1} and a negative band in the amide II region at 1542 cm^{-1} were observed, thus showing that Channelrhodopsin 2 was vertically oriented (Figure 4B). The crucial step was to prove protein activity on the Ni-NTA thiol monolayer. For

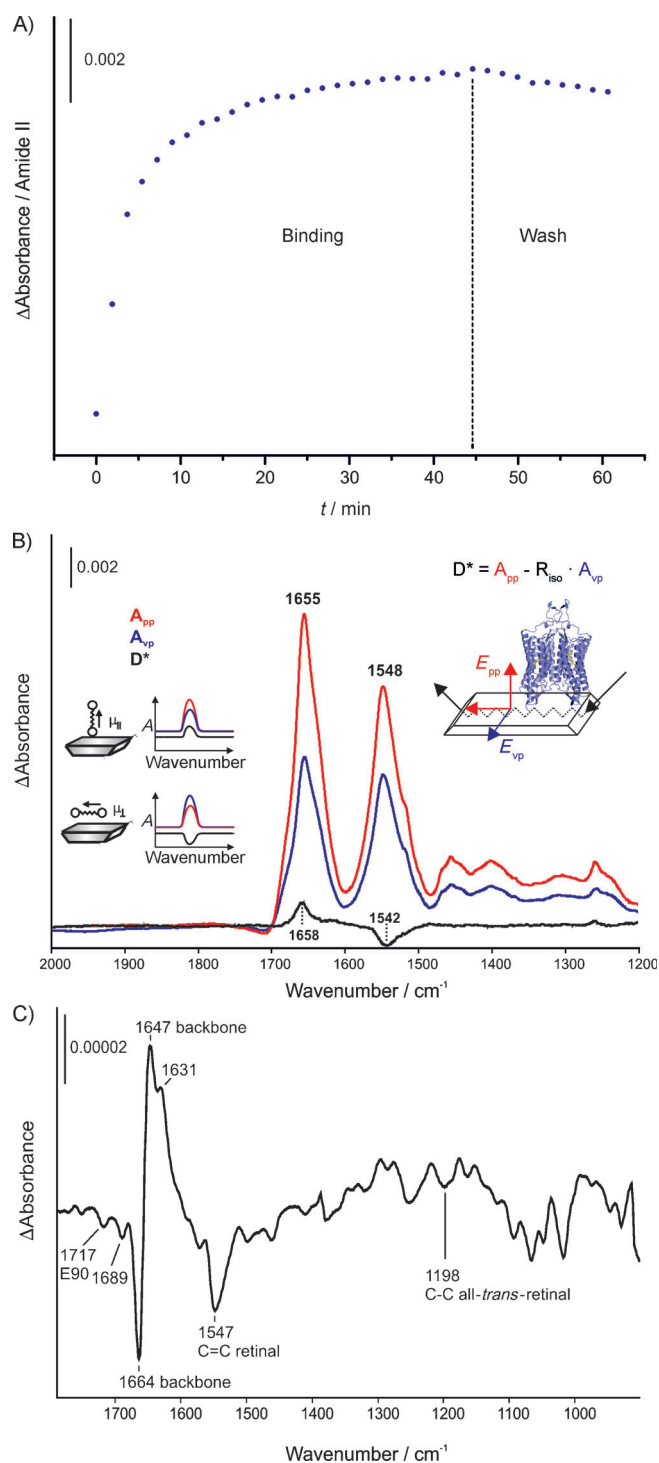


Figure 4. A) Kinetics of the immobilization of Channelrhodopsin 2 on 20% Ni-NTA. B) Polarized spectra of the amide I and II bands were measured with parallel polarized light (red) and vertical polarized light (blue). The dichroic difference spectrum (D^*) was calculated with the given formula from the absorption spectra using parallel (A_{pp}) and perpendicular polarized light (A_{vp}) with the scaling factor R_{iso} . It indicates upright orientation of the α -helices (black). C) Light-induced difference spectrum of immobilized Channelrhodopsin 2 indicates accumulation of the P480 state of the photocycle.

to induce the light-adapted state. A new reference spectrum was recorded after a relaxation time of 2 min, the process was repeated for 14000 scans (4 h), and the data were averaged. The light activated difference spectrum was obtained within a monolayer with an excellent s/n ratio. Positive bands in the spectrum reflect the photostationary state in the photocycle (P480), and the negative bands reflect the dark-adapted state (D470; Figure 4C).^[35] As shown by Eisenhauer et al.,^[35] the negative band at 1717 cm^{-1} corresponds to deprotonation of E90. The large negative band at 1664 cm^{-1} could be caused by changes in carbonyl oscillators near to the retinal binding pocket, as discussed by Neumann-Vorhoeven et al.^[36] We assign the negative band at 1547 cm^{-1} to the retinal carbon double bond and the bands at 1198 cm^{-1} to a carbon single bond of the retinal in its all-trans conformation. The obtained ATR-FTIR difference spectrum is comparable to the FTIR transmission spectrum (Figure S12). Channelrhodopsin 2 showed light-induced activity for over three days. The outstanding quality of the difference spectrum of Channelrhodopsin 2 emphasizes the great potential of our new immobilization method on germanium: much better s/n ratio and reproducibility, in comparison to other techniques like surface-enhanced infrared absorption spectroscopy (SEIRA).^[37]

In conclusion, we report for the first time the chemical functionalization of germanium with thiol chemistry for protein immobilization. Several proteins from different families (transmembrane, membrane-anchored, and soluble proteins) were immobilized by a His-tag and studied by difference spectroscopy. We have filed a patent application (EP14155138.2) regarding its use as a biosensor. Immobilized proteins with reversible reactions like BeF_x binding to Ras-GDP and the photocycle of Channelrhodopsin 2 were shown to be active for several days. The IR difference spectra of the protein monolayers on germanium have an outstanding s/n ratio and allow analysis of the attached proteins in atomic detail. A good s/n ratio can be obtained even for a non-reversible reaction, as demonstrated by the first difference spectrum of the pathogenically relevant phosphocholine transferase AnkX. In addition to protein reactions and protein-ligand interactions, protein-protein interactions and protein orientation can be studied. In principle this approach can be extended to the reconstitution of membrane proteins in lipid bilayers directly on the surface. The great advantage of using thiols in comparison with silanes is that a huge variety of thiols with functional groups for many kinds of protein immobilizations are readily available. In contrast to thiols, surface preparation of silanes has to be done under strict water-free conditions, and a hydrophobic barrier is necessary to form a stable self-assembled monolayer.^[8] Thiol-treated surfaces can be stored for a long time, thus making the measurements more convenient and allowing commercial application. The combination of thiol chemistry with germanium ATR crystals opens new opportunities for the study of immobilized proteins.

Experimental Section

For experimental details, please see the Supporting Information.

this, the flow-through cuvette was equipped with a quartz window, and blue light (463 nm) was applied for 20 s in order

Acknowledgements

We thank Philipp Pinkerneil for preparation of decahistidine-tagged N-Ras1–180 and Kirstin Eisenhauer for preparing the Channelrhodopsin 2 figure. We thank Dr. Jörn Güldenhaupt for helpful discussions and Jens Kuhne for providing the Channelrhodopsin 2 FTIR transmission spectrum. This work was supported by the Deutsche Forschungsgemeinschaft under grant No. SFB 642.

Keywords: ATR-FTIR • biosensors • Channelrhodopsin 2 • germanium • protein immobilization

- [1] S. Waichman, M. Bhagawati, Y. Podoplelova, A. Reichel, A. Brunk, D. Paterok, J. Piehler, *Anal. Chem.* **2010**, *82*, 1478–1485.
- [2] S. Waichman, C. You, O. Beutel, M. Bhagawati, J. Piehler, *Anal. Chem.* **2011**, *83*, 501–508.
- [3] S. Gandor, S. Reisewitz, M. Venkatachalapathy, G. Arrabito, M. Reibner, H. Schröder, K. Ruf, C. M. Niemeyer, P. I. H. Bastiaens, L. Dehmelt, *Angew. Chem. Int. Ed.* **2013**, *52*, 4790–4794; *Angew. Chem.* **2013**, *125*, 4890–4894.
- [4] D. Frenzel, J. M. Glück, O. Brener, F. Oesterheld, L. Nagel-Steger, D. Willbold, *PLoS ONE* **2014**, *9*, e89490.
- [5] S. Locatelli-Hoops, A. A. Yeliseev, K. Gawrisch, I. Gorshkova, *Biomed. Spectrosc. Imaging* **2013**, *2*, 155–181.
- [6] S. Löfås, B. Johnsson, *J. Chem. Soc. Chem. Commun.* **1990**, 1526–1528.
- [7] J. Güldenhaupt, Y. Adigüzel, J. Kuhlmann, H. Waldmann, C. Kötting, K. Gerwert, *FEBS J.* **2008**, *275*, 5910–5918.
- [8] S. Devouge, J. Conti, A. Goldsztein, E. Gosselin, A. Brans, M. Voué, J. De Coninck, F. Homblé, E. Goormaghtigh, J. Marchand-Brynaert, *J. Colloid Interface Sci.* **2009**, *332*, 408–415.
- [9] S. Devouge, C. Salvagnini, J. Marchand-Brynaert, *Bioorg. Med. Chem. Lett.* **2005**, *15*, 3252–3256.
- [10] M. Voué, E. Goormaghtigh, F. Hombé, J. Marchand-Brynaert, J. Conti, S. Devouge, J. De Coninck, *Langmuir* **2007**, *23*, 949–955.
- [11] J. Güldenhaupt, T. Rudack, P. Bachler, D. Mann, G. Triola, H. Waldmann, C. Kötting, K. Gerwert, *Biophys. J.* **2012**, *103*, 1585–1593.
- [12] C. Hammaeher, B. Joris, E. Goormaghtigh, J. Marchand-Brynaert, *Eur. J. Org. Chem.* **2013**, 7952–7959.
- [13] P. Pinkerneil, J. Güldenhaupt, K. Gerwert, C. Kötting, *ChemPhysChem* **2012**, *13*, 2649–2653.
- [14] J. Schartner, J. Güldenhaupt, B. Mei, M. Rögner, M. Muhler, K. Gerwert, C. Kötting, *J. Am. Chem. Soc.* **2013**, *135*, 4079–4087.
- [15] K. Gavriljuk, A. Itzen, R. S. Goody, K. Gerwert, C. Kötting, *Proc. Natl. Acad. Sci. USA* **2013**, *110*, 13380–13385.
- [16] H.-C. Wang, C.-C. Yu, C.-F. Liang, L.-D. Huang, J.-R. Hwu, C.-C. Lin, *ChemBioChem* **2014**, *15*, 829–835.
- [17] L. Yi, Y.-X. Chen, P.-C. Lin, H. Schröder, C. M. Niemeyer, Y.-W. Wu, R. S. Goody, G. Triola, H. Waldmann, *Chem. Commun.* **2012**, *48*, 10829–10831.
- [18] S. Lata, J. Piehler, *Anal. Chem.* **2005**, *77*, 1096–1105.
- [19] K. Ataka, F. Giess, W. Knoll, R. Naumann, S. Haber-Pohlmeier, B. Richter, J. Heberle, *J. Am. Chem. Soc.* **2004**, *126*, 16199–16206.
- [20] K. Ataka, T. Kottke, J. Heberle, *Angew. Chem. Int. Ed.* **2010**, *49*, 5416–5424; *Angew. Chem.* **2010**, *122*, 5544–5553.
- [21] A. Badura, B. Esper, K. Ataka, C. Grunwald, C. Wöll, J. Kuhlmann, J. Heberle, M. Rögner, *Photochem. Photobiol.* **2006**, *82*, 1385–1390.
- [22] M. Lommel, P. Hönicke, M. Kolbe, M. Müller, F. Reinhardt, P. Möbus, E. Mankel, B. Beckhoff, B. O. Kolbesen, *Solid State Phenomena* **2009**, *145–146*, 169–172.
- [23] M. Lommel, F. Reinhardt, P. Hönicke, M. Kolbe, M. Mueller, B. Beckhoff, B. Kolbesen, *ECS Trans.* **2009**, *25*, 433–439.
- [24] T. Hanrath, B. A. Korgel, *J. Am. Chem. Soc.* **2004**, *126*, 15466–15472.
- [25] S. M. Han, W. R. Ashurst, C. Carraro, R. Maboudian, *J. Am. Chem. Soc.* **2001**, *123*, 2422–2425.
- [26] D. Wang, Y.-L. Chang, Z. Liu, H. Dai, *J. Am. Chem. Soc.* **2005**, *127*, 11871–11875.
- [27] J. N. Hohman, M. Kim, H. R. Bednar, J. A. Lawrence, P. D. McClanahan, P. S. Weiss, *Chem. Sci.* **2011**, *2*, 1334–1343.
- [28] M. R. Kosuri, R. Cone, Q. Li, S. M. Han, B. C. Bunker, T. M. Mayer, *Langmuir* **2004**, *20*, 835–840.
- [29] E. Goormaghtigh, V. Raussens, J.-M. Ruyschaert, *Biochim. Biophys. Acta Rev. Biomembr.* **1999**, *1422*, 105–185.
- [30] K. Choi, J. M. Buriak, *Langmuir* **2000**, *16*, 7737–7741.
- [31] J. H. Horton, G. D. Moggridge, R. M. Ormerod, A. V. Kolobov, R. M. Lambert, *Thin Solid Films* **1994**, *237*, 134–140.
- [32] K. Prabhakaran, T. Ogino, *Surf. Sci.* **1995**, *325*, 263–271.
- [33] M. Yang, D. Wouters, M. Giesbers, U. S. Schubert, H. Zuillhof, *ACS Nano* **2009**, *3*, 2887–2900.
- [34] C. Kötting, A. Kallenbach, Y. Suveyzdis, C. Eichholz, K. Gerwert, *ChemBioChem* **2007**, *8*, 781–787.
- [35] K. Eisenhauer, J. Kuhne, E. Ritter, A. Berndt, S. Wolf, E. Freier, F. Bartl, P. Hegemann, K. Gerwert, *J. Biol. Chem.* **2012**, *287*, 6904–6911.
- [36] M.-K. Neumann-Verhoeven, K. Neumann, C. Bamann, I. Radu, J. Heberle, E. Bamberg, J. Wachtveitl, *J. Am. Chem. Soc.* **2013**, *135*, 6968–6976.
- [37] K. Ataka, J. Heberle, *Anal. Bioanal. Chem.* **2007**, *388*, 47–54.

Received: June 18, 2014

Published online on September 24, 2014